

- Landscape position units are universal PMA identification units finer than subbasins.
- A Markov chain-based surrogate model of SWAT+ is developed to identify PMAs.
- SWAT+ is qualified to provide the flow distribution matrix among LSUs and channels.
- LSU-based PMAs are more effective in distribution and cumulative load contribution.
- LSU-based PMAs have general applicability for diverse geographic environments.

1 Identification of watershed priority management areas based on  
2 landscape positions: ~~an~~ An implementation using SWAT+

3  
4 **Highlights**

- 5 ● Landscape position units (~~LSU~~) are ~~adopted~~ universal to identify ~~priority~~  
6 ~~management areas~~ (PMAs) PMA identification units finer than subbasins.
- 7 ● A Markov chain-based surrogate model of SWAT+ is ~~proposed~~ developed to  
8 identify PMAs.
- 9 ● SWAT+ is qualified to provide the flow distribution matrix among LSUs and  
10 channels.
- 11 ● LSU-based PMAs are more effective in distribution and cumulative load  
12 contribution.
- 13 ● LSU-based PMAs have general applicability for ~~various~~ diverse geographic  
14 environments.

15  
16 **Abstract**

17 ~~Priority~~ The priority management areas (PMAs) of a watershed are areas with high  
18 contributions to the pollutant load ~~to~~ of the assessment outlet, such as the watershed  
19 outlet, and, thus, have high priority in the decision -making ~~for~~ of comprehensive  
20 watershed management. Existing spatial units used to identify PMAs are commonly  
21 based on three concepts including subbasins, artificial geographic entities, and grid cells.  
22 However, these identification units cannot balance ~~the~~ general applicability to diverse  
23 geographic environments and the representation degree of spatial heterogeneity, which  
24 impacts the effectiveness of the PMAs. This study proposes ~~adopting~~ utilizing  
25 landscape positions along the hillslope as identification units of PMAs, which can be

26 represented by slope position units (e.g., upland, backslope, and valley). Landscape  
27 position units inherently have upstream-downstream relationships with each other and  
28 with channels. Therefore, their contributions to the assessment outlet can be quantified  
29 based on the propagation effects of hillslope and channel routing processes. The  
30 proposed method was implemented using a restructured and enhanced version of the  
31 Soil and Water Assessment Tool (SWAT<sup>+</sup>) to quantify the pollutants released, and an  
32 improved Markov chain-based surrogate model to distinguish the source contribution  
33 with the improvement of the transition matrix in representing both landscape position  
34 and channel units. Two watersheds, one in China and one in the USA, with different  
35 geographic characteristics were selected to separately conduct ~~the~~ comparative  
36 experiments to identify PMAs at the landscape position and ~~the~~ subbasin levels. The  
37 results showed that PMAs based on landscape positions have more accurate spatial  
38 distribution and require less area for the future configuration of management practices  
39 to achieve the same management goal as PMAs based on subbasins. The better  
40 effectiveness of landscape position units in identifying PMAs is mainly due to their  
41 better ability to represent hillslope processes and the spatial heterogeneity of underlying  
42 surface environments within subbasins. The proposed method can be implemented by  
43 using other watershed models that support landscape position units or different types of  
44 spatial units with explicit upstream-downstream relationships within subbasins.

45 **Keywords:** Priority management areas; Landscape positions; Spatial units;  
46 Pollutant load contribution; Best Management Practices; SWAT<sup>+</sup>

# 1. Introduction

Priority management areas (PMAs) are a prioritizing-prioritized areas for pollution management in the-a watershed, which has a high-pollutant production, and more-importantly,with a high contribution to the pollutant load of its direct or indirect downstream water bodies (Chen et al., 2014). This concept is similar to the-a critical source area (CSA), which is more commonly used to identify highly polluted areas (Pionke et al., 2000; White et al., 2009) but usually does not emphasize propagation effects from upstream to downstream in the watershed, which is essential in-the-for decision-making of-for comprehensive watershed management. Priority management areas are ideal spatial locations for implementing suitable best management practices (BMPs) to effectively control ecological and environmental problems, such as soil erosion and non-point source pollution (Shen et al., 2015; Tian et al., 2020; Guo et al., 2022). The identification of PMAs can be regarded as the first step in the spatial configuration of BMPs for comprehensive watershed management, where factors affecting actual management decisions, such as investment plans, stakeholders<sup>2</sup> willingness, environmental goals, and BMP effectiveness, could-can be considered. The spatial distribution of PMAs considerably affects the locations, areas, and effectiveness of the configured BMPs, affecting the cost-effectiveness of the BMP scenario (i.e., the spatial configuration of multiple BMPs in the watershed) (Chiang et al., 2014; Qin et al., 2018; Wang et al., 2016; Zhu et al., 2021). Therefore, the accurate identification of PMAs is a key issue for comprehensive watershed management (Chen et al., 2022).

22 The ~~foremost~~ important step in identifying PMAs is to determine an appropriate  
23 type of spatial units as a computing unit for pollutant production and contribution to the  
24 assessment outlet, such as the watershed outlet (hereafter referred to as the  
25 identification units) (Dong et al., 2018; White et al., 2009). The identification units  
26 ~~adopted~~ utilized in existing research are mainly based on three concepts: subbasins  
27 (Shang et al., 2012; Chen et al., 2014; Shen et al., 2015; Dong et al., 2018), artificial  
28 geographic entities (Tian et al., 2020), and grid cells (Kovacs et al., 2012).

29 ~~The~~ A subbasin represents a relatively closed and independent geographic unit that  
30 is linked to other subbasins through channels. Subbasin units are the most  
31 straightforward and ~~most~~ frequently used identification units because they are  
32 delineated and modeled in most watershed modeling. In addition to directly utilizing  
33 subbasin units, researchers also use the combination of subbasins as identification units  
34 according to administrative regions (such as villages; Shang et al., 2012), for the benefit  
35 of making and implementing watershed management policies, especially in large study  
36 areas (Liu et al., 2019; Shang et al., 2012). However, a subbasin can be recognized and  
37 modeled as an integral of one or more levels of finer spatial units to better represent  
38 spatial heterogeneity within ~~#the~~ subbasin, such as hillslopes, slope position units,  
39 landuse fields, and even grid cells. Therefore, it may be too coarse to use these subbasin-  
40 based identification units because the heterogeneity of pollutant sources and  
41 transportation processes within the subbasins should be considered (Qin et al., 2018;  
42 Wang et al., 2016).

43 Artificial geographic entities refer to artificially constructed and hydrologically

44 connected geographic entities based on the characteristics of a specific geographic  
45 environment (Ghebremichael et al., 2013), such as polders that developed in lowland  
46 plains with densely distributed rivers and lakes (Tian et al., 2020). Such spatial units  
47 have relatively homogeneous features from the perspectives of physical geographic  
48 processes and/or anthropogenic activities. For example, a polder may contain  
49 agricultural land, irrigation channels, ponds, and even villages, that are enclosed by  
50 artificial dams to serve as conservation areas for flood [management](#) and waterlogging.  
51 Although artificial geographic entities are appropriate for use as identification units  
52 [than subbasins](#) in the corresponding geographic environments, they are not ~~easy to be~~  
53 generalized as ~~generally applicable~~[universal](#) identification units and, ~~thus, are cannot~~  
54 [be](#) widely applied ~~to in most~~[diverse geographic environments](#).

55 Grid cells are commonly used spatial units with regular shapes in geographic  
56 modeling, and their underlying surface characteristics are homogeneous. [Grid cells are](#)  
57 [universal units to identify PMAs accurately](#) ~~u~~Using [those](#) watershed models that  
58 explicitly represent flow routings among grid cells, ~~PMAs can be identified accurately~~  
59 (Kovacs et al., 2012). However, using grid cells may cause more fragmented  
60 distributions of PMAs, which reduces the implementation efficiency and limits further  
61 application (e.g., ~~the for~~ PMA-based spatial optimization of BMPs).

62 Therefore, the existing spatial units used for identifying PMAs cannot balance ~~the~~  
63 general applicability to diverse geographic environments and the representation degree  
64 of spatial heterogeneity. According to the ~~previous~~[foregoing](#) analysis, proper  
65 identification units should (1) be broadly available and not be limited to a specific

66 geographic environment; (2) be capable of representing the spatial heterogeneity of  
67 underlying surface characteristics, physical geographic processes, and/or  
68 anthropogenic activities inside the study area by a small number of units; and (3) have  
69 hydrologic connections among each other.

70 This study proposes the use of landscape positions along hillslopes within each  
71 subbasin to identify PMAs. In this study, landscape positions refer to the geographic  
72 objects –can be delineated by landform units (also referred to as slope position units)  
73 that reflect the integrated effects of hillslope processes on topography and affect  
74 geographic processes on the surface (Volk et al., 2007; Arnold et al., 2010; Miller and  
75 Schaetzl, 2015; Qin et al., 2018). Landscape position units are universality in most  
76 geographic environments that can be delineated by slope position units (Wolock et al.,  
77 2004; Volk et al., 2007; Qin et al., 2009). Based on commonly used classification  
78 systems of slope positions (e.g., the divide, backslope, and valley units adopted-utilized  
79 by Arnold et al. (2010)), each subbasin needs only a few spatial units (e.g., three) to  
80 represent the spatial homogeneity from the perspective of hillslope processes (Qin et  
81 al., 2018; Rathjens et al., 2016). In addition, landscape position units have inherent  
82 upstream-downstream relationships among each other, which have been considered in  
83 watershed modeling (Arnold et al., 2010; Bieger et al., 2019; Rathjens et al., 2015; Yang  
84 et al., 2002) and spatial optimization of BMPs (Qin et al., 2018; Zhu et al., 2019; Zhu  
85 et al., 2021). Thus, landscape position units meet the requirements for use as the  
86 aforementioned identification units mentioned above.

87 This study proposes a PMA identification method based on landscape position

88 units exemplified by SWAT<sup>+</sup> (i.e., the restructured and enhanced version of the Soil and  
89 Water Assessment Tool) and evaluates the effectiveness of the proposed method by  
90 comparing it to widely used subbasin units. The remainder of this paper is organized as  
91 follows: Section 2 introduces the proposed method; and Section 3 presents a  
92 comparative experimental design of using landscape position and subbasin units to  
93 identify PMAs of total nitrogen in two watersheds with different geographic  
94 characteristics. The experimental results and discussion are presented in Section 4, and  
95 the conclusions are presented in Section 5.

## 96 **2. Method design**

97 To identify PMAs at the landscape position unit level, two key issues must be  
98 addressed. The first is the quantification of pollutants released ~~at~~ [from the](#) landscape  
99 position units. The second is how to distinguish the pollutant load contribution of each  
100 landscape position unit to the assessment outlet, that is, the residual amount of pollutant  
101 after being transported to its direct downstream channel and then transitioning in  
102 hierarchical channels before reaching the assessment outlet (Chen et al., 2014).

103 Generally, the contribution of the pollutant load cannot be directly determined  
104 from the results of most watershed models. Instead, watershed models output the  
105 pollutant released from each simulation unit (e.g., the hydrologic response unit [HRU]  
106 in SWAT) or lumped unit (e.g., subbasin), as well as the flow of substances in and out  
107 of each channel. To fill this gap, Grimvall and Stålnacke (1996) proposed a Markov  
108 chain-based surrogate model to simulate pollutant transitions from upstream channels



109 (one channel for each subbasin) to the assessment outlet in a statistical manner. Their  
110 basic idea is to use analog pollutant transformation and transfer processes in  
111 hierarchical channels as a Markov process, in which, the transition matrix is determined  
112 by the upstream-downstream relationships among channels and the retention effects of  
113 the channel routing process. After a finite number of transitions (equal to the length of  
114 the longest branch in hierarchical channels), all pollutants from upstream subbasins  
115 reach the assessment outlet, thus, the corresponding pollutant load contributions can be  
116 derived (Grimvall and Stålnacke, 1996).

117 Follow-up studies continued to ~~adopt~~ apply the subbasin unit in the Markov chain-  
118 based model (Chen et al., 2014; Rankinen et al., 2016), which includes pollutant  
119 production ~~on~~ hillslopes and pollutant routing in the channel. The transition matrix of  
120 the Markov chain-based model can be improved to represent both landscape position  
121 and channel units. Therefore, if ~~we can separate~~ these two processes can be separated  
122 in the landscape position units and channels, the improved Markov chain-based model  
123 will be able to distinguish the pollutant contribution of each landscape position unit to  
124 the assessment outlet. Based on this basic idea, the proposed method aims to incorporate  
125 a watershed model that supports landscape position units as simulation or lumped units,  
126 to improve the Markov chain-based PMA identification method from the subbasin level  
127 to the landscape position unit level. Therefore, the Markov chain-based PMA  
128 identification method can be generalized as a method framework that supports one or  
129 more types of hierarchical spatial units with explicit hydrological connections (i.e.,  
130 upstream-downstream relationships), such as subbasins and landscape position units

131 (Fig. 1).

## 132 **2.1 Delineation and modeling of landscape position units in SWAT<sup>+</sup>**

133 As a restructured and enhanced version of the SWAT model, SWAT<sup>+</sup> (Bieger et al.,  
134 2017, 2019) introduced a new type of spatial unit between the subbasin unit and HRU  
135 named the landscape position unit (LSU), which includes the uplands and floodplains  
136 (Fig. 2). SWAT<sup>+</sup> uses the relative position index (RPI) of each cell in a gridded digital  
137 elevation model (DEM) to delineate LSUs (Rathjens et al., 2016). The RPI of each cell  
138 is the ratio of the drop length to its downstream valley (i.e., the stream cell) and the  
139 length from its upstream ridge cell to the same valley cell. The RPI ranges from 0 to 1.  
140 The cell with a RPI less than the user-specific threshold is classified as the floodplain.

141 This means that the basic spatial discretization of a watershed in SWAT<sup>+</sup> contains three  
142 types of nested spatial units as a hierarchy: subbasin, LSU, and HRU. The HRU, as the  
143 basic simulation unit of SWAT<sup>+</sup>, is delineated as the unique combination of soil, land  
144 use, and slope class within the LSU, which is spatially discrete (Fig. 2a) and even lacks  
145 explicit spatial locations according to different delineation parameters. Therefore,  
146 HRUs are unsuitable for PMA identification units since there are no hydrologic  
147 connections between HRUs, although the HRU is finer than the LSU. In addition,  
148 SWAT<sup>+</sup> also abstracts specific types of geographic entities as spatial units with locations  
149 and properties to participate in watershed modeling. For example, reservoirs or ponds  
150 within a subbasin are first generalized as one point in the channel that divides the  
151 channel into two parts, and then defined by the upstream part with additional properties  
152 such as storage capacity (Fig. 2a). The hillslopes, LSUs, and HRUs also are ~~also~~

153 delineated accordingly, while the two aquifer units remain unchanged (Fig. 2b). These  
154 spatial units can enrich the flow routing network of SWAT<sup>+</sup> and play important roles in  
155 the simulation of study areas with specific geographic environments, such as,  
156 agricultural ecosystems with densely distributed ponds.

157 With the new spatial discretization scheme, SWAT<sup>+</sup> ~~improved~~improves the  
158 representation of realistic hydrologic processes from hillslopes to channels (Bieger et  
159 al., 2019). Instead of directly adding all released substances ~~of from~~from HRUs (including  
160 water, sediment, and pollutants) to the channel, SWAT<sup>+</sup> first lumps HRUs' outputs at  
161 the LSU level and then routes these outputs to other spatial units using two different  
162 methods. The first method involves completely draining from the upland to the  
163 floodplain and from the floodplain to the channel, which is applicable for lateral flow  
164 in soils and groundwater recharge in aquifers (Fig. 2b). The second method distributes  
165 water from the upland to the channel/pond/reservoir by a constant ratio (e.g., 0.30 from  
166 LSU2 to the pond and 0.66 from LSU4 to the channel, as shown in Fig. 2b; hereafter  
167 'channel/pond/reservoir' is referred to as channel collectively) and the rest to the  
168 floodplain as additional net precipitation to participate in the hydrologic simulation.  
169 The output from the floodplain drains entirely into the channel (Fig. 2b). SWAT<sup>+</sup>  
170 provides two ways to determine this ratio: the user-specified global value for all upland  
171 units in the watershed and the area ratio of each upland to its floodplain. The area ratio  
172 method has been proven to be more realistic in representing the connectivity than the  
173 fixed ratio for the entire watershed (Bieger et al., 2019) and is, therefore, ~~adopted~~  
174 applied in this study.

175 With the flow routing network primarily constructed by [chain of](#) HRU, LSU, and  
 176 channel (Fig. 2b), SWAT<sup>+</sup> is ~~qualified~~-[suitable](#) to quantify pollutants released at [the](#)  
 177 landscape position units and the corresponding transportation amounts to their direct  
 178 channels.

## 179 **2.2 Pollutant load contribution of landscape position units derived** 180 **from a Markov chain-based surrogate model of SWAT<sup>+</sup>**

181 Based on the flow routing network and simulation results of SWAT<sup>+</sup>, the key part  
 182 of the Markov chain-based surrogate model can be determined, that is, the transition  
 183 matrix of pollutants through LSUs and channels. Subsequently, using the lumped  
 184 simulation results at LSUs as inputs, the Markov chain-based model can determine the  
 185 pollutant load contribution of each landscape position unit.

### 186 **2.2.1 Transition matrix of pollutants based on flow routing network and retention** 187 **effects of [the](#) channel routing process**

188 The transition matrix is constructed using flow distribution relationships from  
 189 upstream to downstream units and the retention coefficients of channel routing  
 190 processes (Chen et al., 2014). According to the spatial discretization scheme of SWAT<sup>+</sup>  
 191 (see Section 2.1), the flow distribution relationships among the LSUs and channels can  
 192 be represented by an  $n \times n$  matrix  $H$  (Eq. 1). Fig. 3 shows an example of the matrix  $H$ .

$$193 \quad H(i,j) = \begin{cases} s, & \text{if LSU (floodplain) } j \text{ is adjacent downstream of LSU (upland) } i \\ 1-s, & \text{if CHA (channel) } j \text{ is directly downstream of LSU (upland) } i \\ 1, & \text{if CHA } j \text{ is adjacent downstream of CHA } i \text{ or LSU (upland) } i \\ 0, & \text{otherwise} \end{cases} \quad (1)$$

194 where  $n$  is the total number of LSUs and channels in the watershed, and  $s$  is the flow

195 distribution ratio from upland to floodplain. For surface runoff,  $s$  is initially set by the  
196 area ratio of upland and hillslope, while for lateral flow and groundwater recharge,  $s =$   
197 1 (Fig. 2b). Each row represents the flow distribution relationships of a spatial unit with  
198 its downstream units. The sum of all elements in one row equals 1, except for the  
199 channel row where the assessment outlet is located (e.g., the 7<sup>th</sup> row in Fig. 3, when the  
200 outlet of channel 7 is the assessment outlet). For a given assessment outlet of channel  
201  $k$ , there exists a smallest integer  $N_k$  to make  $H^{N_k} = 0$ , which means that after  $N_k$   
202 transitions, pollutants from all upstream spatial units of channel  $k$  will reach the outlet.  
203 The physical meaning of  $N_k$  is the longest routing length from the uppermost spatial  
204 units to the outlet of channel  $k$ , for example,  $N_7 = 4$  in Fig. 3.

205 The complicated channel routing process of pollutants accounts ing for the  
206 chemical pollutant transformation or retardation of the interested substances. For  
207 example, a stepwise transformation from organic nitrogen to ammonia, then to nitrite,  
208 and finally to nitrate is simulated in SWAT (Neitsch et al., 2011). For each channel of  
209 the study area, the difference between the output substance and the input can be  
210 explained by the retention effect of the channel, which is time-varying and affected by  
211 pollutant concentration, water temperature, and other factors. The yearly average  
212 retention of each channel and transfer processes can be regarded as its stable removal  
213 capacity of pollutants calculated as simplified by using a the retention coefficient (Eq.  
214 2) (i.e., removal capacity of pollutants) as a surrogate calculation method (Chen et al.,  
215 2014; Grimvall and Stålnacke, 1996; Hejzlar et al., 2009). The landscape position unit  
216 is a lumped unit of pollutant sources calculated at HRUs, thus, it has no retention effect.

217 
$$r = (\text{Load}_{\text{in}} - \text{Load}_{\text{out}}) / \text{Load}_{\text{in}} \quad (23)$$

218 where  $r$  denotes the retention coefficient of the channel to a specific pollutant;  $\text{Load}_{\text{in}}$   
 219 is the pollutant input to the channel- $j$  that includes pollutant outputs of adjacent  
 220 upstream channels and pollutant released from upstream LSUs; and  $\text{Load}_{\text{out}}$  is the  
 221 pollutant output at the outlet of the channel- $j$ .

222 The retention coefficient of spatial units,  $R$ , also is also represented by an  $n \times n$   
 223 matrix, as follows:

224 
$$R = \begin{pmatrix} r_1 & 0 & \cdots & 0 \\ 0 & r_2 & \cdots & 0 \\ \vdots & \vdots & \ddots & \vdots \\ 0 & 0 & \cdots & r_n \end{pmatrix} \quad (32)$$

225 Where where the  $i$ th diagonal element  $r_i$  denotes the retention coefficient of spatial unit  
 226  $i$ ; for LSUs,  $r_i = 0$ ; and for channels,  $r_i$  can be calculated using Eq. 2 the simulation  
 227 results of for the channels:

228 
$$r_j = (\text{Load}_{\text{in}} - \text{Load}_{\text{out}}) / \text{Load}_{\text{in}} \quad (3)$$

229 where  $\text{Load}_{\text{in}}$  is the pollutant input to channel- $j$  that includes pollutant outputs of  
 230 adjacent upstream channels and pollutant released from upstream LSUs; and  $\text{Load}_{\text{out}}$  is  
 231 the pollutant output at the outlet of channel- $j$ .

232 The transition matrix,  $\tilde{H}$ , of the Markov chain-based model can be represented  
 233 as follows and used to simulate the flow transitions of substances (e.g., water and  
 234 pollutants) through the hierarchy of landscape position units and channels:

235 
$$\tilde{H} = H (I - R) \quad (4)$$

236 where  $I$  is an identity matrix.

237 **2.2.2 Calculation of pollutant load contribution**

238 Except for the transition matrix, the pollutant released from each LSU is the  
 239 primary input data for the Markov chain-based model as the initial states. Because the  
 240 channel acts as a receptor for pollutants, it contains no self-generated pollutants. An  $n$   
 241  $\times 1$  matrix,  $L$ , is used to organize the input of the pollutant sources:

$$242 \quad L = (e_1, e_2, \dots, e_i, \dots, e_n)^T \quad (5)$$

243 where  $e_i$  is the pollutant released from spatial unit  $i$  based on the simulation results of  
 244 SWAT<sup>+</sup>. Specifically,  $e_i = 0$ , if  $i$  is a channel.

245 The pollutant load contribution of each spatial unit to a specific assessment outlet  
 246 can be calculated using simple matrix calculations (Grimvall and Stålnacke, 1996):

$$247 \quad E = (\tilde{H}_k)^{N_k} V_k * L \quad (6)$$

$$248 \quad \tilde{H}_k(i, j) = \begin{cases} \tilde{H}(i, j), & \text{if } i \neq k \\ 1, & \text{if } i = j = k \\ 0, & \text{if } i = k \text{ and } j \neq k \end{cases} \quad (7)$$

$$249 \quad V_k(i) = \begin{cases} 1, & \text{if } i = k \\ 0, & \text{otherwise} \end{cases} \quad (8)$$

250 where  $k$  represents the assessment outlet located channel, and the corresponding  
 251 modification from  $\tilde{H}$  to  $\tilde{H}_k$  implies that the  $k$ th state is transformed to an absorbing  
 252 state;  $V_k$  is an  $n \times 1$  matrix for extracting the  $k$ th column of the  $(\tilde{H}_k)^{N_k}$ , resulting in  
 253 the contribution rate of each unit; and the asterisk\* denotes element-wise  
 254 multiplication.

255 Considering that the pollutants of interest may have various states that are modeled  
 256 in different watershed processes, the calculation of the pollutant load contribution

257 should be combined with all components calculated by different transition matrixes,  $H$ ,  
 258 and pollutant source matrixes,  $L$ . For example, the total nitrogen consists of organic and  
 259 inorganic nitrogen. In SWAT/SWAT<sup>+</sup>, the inorganic nitrogen output in the channel  
 260 includes ammonia, nitrite, and nitrate nitrogen. The considered in this study mainly  
 261 includes nitrate nitrogen ( $NO_3$ ) and the organic nitrogen ( $ORGN$ ) are relatively stable  
 262 forms of nitrogen in the soil that are routed from HRUs into the channel with water and  
 263 sediment (Neitsch et al., 2011). Since the nitrogen output at the LSU level is the sum of  
 264 its internal HRUs' output, the nitrogen released from LSUs considered in this study also  
 265 comprises  $NO_3$  and  $ORGN$ . For the sake of simplicity, we use the term of total nitrogen  
 266 (TN) in this study. The TN total nitrogen load contribution can be calculated as follows:

$$267 \quad E_{TN} = E_{NO_3-SURF} + E_{NO_3-LAT} + E_{NO_3-GW} + E_{ORGN} \quad (9)$$

$$268 \quad E_{NO_3-SURF} = (H_{SURF} (I - R_{NO_3})_k)^{N_k} V_k * L_{NO_3-SURF} \quad (10)$$

$$269 \quad E_{NO_3-LAT} = (H_{LAT} (I - R_{NO_3})_k)^{N_k} V_k * L_{NO_3-LAT} \quad (11)$$

$$270 \quad E_{NO_3-GW} = (H_{GW} (I - R_{NO_3})_k)^{N_k} V_k * L_{NO_3-GW} \quad (12)$$

$$271 \quad E_{ORGN} = (H_{SURF} (I - R_{ORGN})_k)^{N_k} V_k * L_{ORGN-SURF} \quad (13)$$

272 where  $SURF$  denotes the surface runoff,  $LAT$  denotes the lateral flow,  $GW$  denotes the  
 273 groundwater recharge;  $H_{SURF}$ ,  $H_{LAT}$ , and  $H_{GW}$  describe the flow distribution  
 274 relationships among the spatial units of surface runoff, lateral flow, and groundwater  
 275 recharge, respectively;  $L_{NO_3-SURF}$ ,  $L_{NO_3-LAT}$ , and  $L_{NO_3-GW}$  are the amounts of  $NO_3$  released  
 276 in surface runoff, lateral flow, and groundwater recharge, respectively; and  $L_{ORGN-SURF}$   
 277 is the amount of  $ORGN$  released in surface runoff.



### 278 2.2.3 PMA identification based on classification of pollution degrees

279 Once the pollutant load contribution of each landscape position unit is  
280 distinguished, a classification of pollution degrees can be ~~adopted~~determined to  
281 identify different levels of PMAs, such as high-, medium-, and low-contribution PMAs.  
282 ~~The classification methods in existing studies include the natural breaks method,~~  
283 ~~standard deviation method, and water quality control targets method (Chen et al., 2014;~~  
284 ~~Giri et al., 2016).~~ In this study, we adopted the natural breaks method, a commonly used  
285 classification method (De Smith et al., 2018; Giri et al., 2016), to classify the pollutant  
286 load contribution. The natural breaks method classifies the data into different classes  
287 with the statistical groupings and pattern characteristics inherent in the data to minimize  
288 the data difference within a class and maximize the difference between classes.

## 289 3. Experimental design

290 To illustrate the effectiveness of the proposed method, a comparative experimental  
291 study was designed to identify the PMAs ~~of~~for total nitrogen at the landscape position  
292 and subbasin levels based on the same calibrated SWAT<sup>+</sup> model. The source of total  
293 nitrogen considered in this study is summed by nitrate nitrogen and organic nitrogen on  
294 the LSU. Since the improvement of the Markov-based surrogate model in this study  
295 does not change the calculation principle of the original model, the differences in  
296 identifying PMAs can be attributed to the identification units adopted (i.e., the LSU and  
297 the subbasin unit). The same experimental design was used in two watersheds to  
298 evaluate the applicability of the method under different geographic characteristics (e.g.,

299 topographical, climatic, hydrological, and ecological conditions), that is, the  
300 Zhongtianshe Watershed (~42 km<sup>2</sup>) in southern China and the Willow River Watershed  
301 (~212 km<sup>2</sup>) in western Wisconsin, USA (Fig. 4).

### 302 **3.1 Study areas and data**

303 The Zhongtianshe Watershed, located ~~in the~~ south of Liyang ~~City~~, Jiangsu  
304 Province, China, is a typical hilly area situated in the upstream region of Lake Tai. The  
305 study area is characterized by a subtropical monsoon climate. The average annual  
306 temperature is 15.5°C and the average annual precipitation is 1160 mm. The main soil  
307 type is yellow-red soil, which is a type of acidic soil that is easily weathered. The main  
308 land use types ~~were~~ are forests (77%), croplands (10%, primarily rice paddy fields),  
309 orchards (3%), residential areas (8%), and water areas (2%). The watershed experiences  
310 frequent agricultural activities, and the cultivation of rice and wheat is the primary  
311 contributor to local non-point source pollution. Because the study area is ~~on~~ in the  
312 drinking water source of Liyang, knowing the details of the pollution situation and  
313 taking reasonable measures to control pollution is a vital issue for the local government  
314 (Shi et al., 2021).

315 The Willow River, located in western Wisconsin, USA, is a tributary of the St.  
316 Croix River. It is classified as part of the Central Wisconsin Undulating Till Plain based  
317 on a report by the U.S. environmental ~~Environmental protection~~ Protection agency  
318 Agency (EPA, 2020), and is characterized as relatively flat compared to the  
319 Zhongtianshe watershed. The area has a continental climate with high  
320 evapotranspiration, an average annual temperature of 11.8°C, and an average annual

321 precipitation of 788 mm. The soils are predominantly silt loams with moderately well-  
322 drained characteristics. The main land use types ~~were~~are grasslands (45%), forests  
323 (27%), croplands (18%), residential areas (6%), and wetlands (3%). Watershed crops  
324 are dominated by corn-silage, soybeans, and alfalfa, resulting in non-point source  
325 pollution and relatively poor water quality. As the headwater of the popular Willow  
326 River State Park and attractive trout fishing destinations, the watershed has been the  
327 focus of non-point source pollution control for decades (Almendinger and Murphy,  
328 2007).

329 The input data of the study areas for the SWAT<sup>+</sup> modeling consisted of a digital  
330 elevation model (DEM), land use types, soil types and properties, meteorological data,  
331 agricultural management practices, and observed data at the watershed outlet. Detailed  
332 descriptions of the data for the two watersheds are ~~presented~~listed in Table 1.

### 333 **3.2 Modeling and calibration of the SWAT<sup>+</sup> model**

334 Two SWAT<sup>+</sup> models (~~version 59.3~~) were built by QSWAT<sup>+</sup> version 1.2.2 and  
335 SWAT<sup>+</sup> version 59.3 –to simulate the total nitrogen pollution in each study area. A total  
336 of 15 subbasins, 41 LSUs, and 1260 HRUs were generated in the Zhongtianshe  
337 Watershed, while 19 subbasins, 131 LSUs, and 7245 HRUs were generated in the  
338 Willow River Watershed (Fig. 5). The RPI thresholds for delineating uplands and  
339 floodplains were manually determined by visual interpretation of contour lines, which  
340 are 0.14 and 0.3 for the Zhongtianshe Watershed and the Willow River Watershed,  
341 respectively. In most situations, each subbasin has one upland and one floodplain. There  
342 may be an additional floodplain due to the very short channel generated after the setting

343 of a pond or reservoir.

344 Limited by the available observed data ~~of~~for the Zhongtianshe Watershed, ~~we set~~  
345 the year 2011 was set as a warm-up period, and 2012–2013 and 2014–2015 were set as  
346 calibration and validation periods, respectively, for daily flow modeling. The model  
347 performance ~~of~~for the total nitrogen was calibrated using the only 5-day or 3-day  
348 monitoring data from 2014 to 2015 (a total of 181 values, of which 53 values during  
349 the rainy season were sampled in about three days interval from June to August in the  
350 two years), without validation.

351 For the Willow River ~~watershed~~Watershed, the model had a 2-year warm-up  
352 period. The calibration period ranged from 1 January 2012 to 31 July 2014, and the  
353 validation period was from 1 October 2010 to 31 December 2011, respectively. The  
354 available daily ammonia and organic nitrogen were combined to calibrate and validate  
355 the nitrogen modeling.

356 Model performance was evaluated using the Nash–Sutcliffe efficiency (NSE,  
357 Nash and Sutcliffe, 1970), percentage bias (PBIAS), root mean square error-standard  
358 deviation ratio (RSR), and coefficient of determination ( $R^2$ ), as listed in Table 2.  
359 According to the criteria of monthly model performance proposed by Moriasi et al.  
360 (2007), a satisfactory model should generally have the NSE > 0.50, RSR < 0.70, and  
361 PBIAS  $\pm$ 25% for flow,  $\pm$ 55% for sediment,  $\pm$ 70% for nutrients. ~~calibrated SWAT+~~  
362 ~~models have approximately satisfactory performance for flow modeling in both study~~  
363 ~~areas. For nitrogen, considering that a shorter time step may~~ Meanwhile, the daily  
364 model is more likely to ~~cause~~have poorer model performance than the monthly model

365 (Engel et al. 2007), ~~and that the simulation trends represented by  $R^2$  have good (shown~~  
366 ~~in  $R^2$ ) was quite consistency with the observed data.~~ Therefore, considering this study  
367 mainly utilizes the relative rather than absolute reliable model results to verify the  
368 effectiveness of the proposed PMA identification method, both calibrated models can  
369 be regarded as acceptable ~~are applicable for the validation of the proposed PMA~~  
370 ~~identification method in this study.~~ Besides, considering the SWAT<sup>+</sup> is still in active  
371 development, we created an open-source repository to store the modeling data and  
372 update the modeling details and results routinely in our following study  
373 (<https://github.com/lreis2415/WatershedModelingData>).

### 374 **3.3 Identification and evaluation of PMAs at LSU level and subbasin** 375 **level**

376 To evaluate the effectiveness of the PMAs at the LSU level, PMAs also were ~~also~~  
377 identified at the subbasin level in the same study area based on the same calibrated  
378 SWAT<sup>+</sup> model and the ~~original~~ Markov chain-based surrogate model.

379 The average annual total nitrogen modeled during the calibration period was used  
380 for the input data of the Markov chain to identify the PMAs, with the watershed outlet  
381 set as the assessment outlet. The natural breaks s method was ~~adopted~~ utilized to classify  
382 the nitrogen load contribution of the spatial units into three classes, and high-  
383 contribution areas were identified as PMAs.

384 The comparison of the PMAs identified at the LSU and subbasin levels was  
385 ~~conducted~~ done from two perspectives, the spatial distribution and cumulative load  
386 contributions. The spatial distribution of PMAs is an intuitive way to qualitatively

387 analyze the spatial consistency and differences between different units. The cumulative  
388 load contributions were used to quantitatively compare the relationships between the  
389 areas of PMAs and their total pollutant load contribution.

## 390 **4. Experimental results and discussion**

### 391 **4.1 Spatial distribution of PMAs**

392 In the Zhongtianshe Watershed, five LSUs and two subbasins, classified as high-  
393 contribution areas, were identified as PMAs (Fig. 6). There was a relatively consistent  
394 spatial correlation between the two levels. For example, one subbasin was identified as  
395 PMA at both levels, that is, subbasin S2 in Fig. 6b and its two LSUs, L2 and L3 in Fig.  
396 6a. PMAs identified at the LSU level ~~had~~have a more accurate spatial distribution  
397 because of the inherent characteristics of the LSUs that can represent the spatial  
398 heterogeneity within subbasins. Considering the retention effect of ponds and reservoirs  
399 in SWAT<sup>+</sup>, the upstream part of the subbasin may have a distinctive load contribution  
400 compared to the downstream part. For example, in ~~the~~ subbasin S1 in Fig. 6b, the  
401 upstream part ~~constituted by~~composed of floodplain L10 and upland L12 in Fig. 6a  
402 were identified as medium-contribution areas, while the downstream floodplain L1 was  
403 the high-contribution area. In addition, most LSU-based PMAs were floodplains in the  
404 Zhongtianshe Watershed. This may be because ~~that~~ the cropland in the study area is  
405 mostly distributed along the valley plain, which is a direct cause of local non-point  
406 source pollution. These results also ~~prove~~indicate that SWAT<sup>+</sup> is well suited for  
407 characterizing pollutants released at the LSU level and their transitions in the

408 reconstructed routing network by LSUs and channels (including ponds).

409 In the Willow River Watershed, two LSUs and two subbasins, classified as high-  
410 contribution areas, were identified as PMAs (Fig. 7). It was similar that at both the LSU  
411 and subbasin levels ~~where~~ the northeast areas of the watershed were identified as low  
412 contribution areas, owing to the upstream pollution predominantly reduced by the  
413 ponds and wetlands along the main channel. Although the results identified at the two  
414 levels had similar spatial distributions, the subbasin-based PMAs covered larger areas  
415 than the LSU-based PMAs, which may result in additional screening work or more  
416 investment in watershed management decision-making. In contrast, the LSU-based  
417 PMAs were the upland areas within the subbasins, that is, uplands L1 and L2 (Fig. 7a)  
418 within two subbasins (Fig. 7b). The medium-contribution areas identified at the LSU  
419 level were also more specific and detailed than the areas identified at the subbasin level.  
420 Therefore, it is clear that LSU-based results can provide a finer identification than  
421 subbasin-based results in the Willow River Watershed.

422 In addition, for the Willow River Watershed, LSUs belonging to subbasin L2 in  
423 Fig. 7b were not identified as PMAs but as contribution areas ~~below~~ classified as  
424 medium-contribution areas. This shows that the application of detailed spatial units  
425 could decompose the aggregation of the pollutant load within a subbasin in a relatively  
426 realistic representation, although subbasin S2 contributed a high pollutant load as the  
427 result of being the largest subbasin in the watershed.

428 Overall, LSU-based PMAs have improved the accuracy of identification from the  
429 perspective of spatial distribution compared with subbasin-based PMAs. It is also

430 ~~proven~~ shown that the proposed PMA identification method at landscape position units  
431 using SWAT<sup>+</sup> is effective and applicable to different watersheds.

## 432 **4.2 Cumulative load contribution**

433 To quantitatively evaluate the difference in PMAs identified at the LSU and  
434 subbasin levels for each case study, each type of spatial unit was ranked by load  
435 contribution in descending order and plotted in Figs. 8 and 9, with the cumulative area  
436 and load contribution calculated.

437 In the Zhongtianshe Watershed, LSU-based PMAs contributed 48.6% of the total  
438 nitrogen in 23.3% of the watershed area, whereas subbasin-based PMAs only  
439 contributed 44.7% in as much as 30.1% of the area (Fig. 8a). This means that landscape  
440 position units are more effective in identifying the PMAs. Moreover, the cumulative  
441 area-contribution line of the LSU-based method in Fig. 8a was always higher than that  
442 of the subbasin-based method, proving its better effectiveness, although based on  
443 different types of identification units.

444 In the Willow River Watershed, LSU-based PMAs contributed 31.7% of the total  
445 nitrogen in 5.9% of the watershed area, whereas subbasin-based PMAs contributed 54.9%  
446 of the total nitrogen in 21.5% of the area (Fig. 9a). It is not convincing to simply use  
447 these numbers to compare the effectiveness of the two levels in this watershed.  
448 However, the line in Fig. 9a shows that the LSU-based PMAs almost always covered  
449 less area than the subbasin-based PMAs under the same cumulative contribution. In  
450 general, the results revealed that there would be less work on the reduction of pollution  
451 at the LSU level if the local government wanted to control the pollution to a certain



452 extent.

453 Furthermore, there was no deterministic relationship between the area of the  
454 spatial unit and its pollutant load contribution. For example, LSU L1 in the  
455 Zhongtianshe Watershed contributed 12.0% of the total nitrogen but ranked 17 in area,  
456 while subbasin S1 contributed 24.3% of the total nitrogen with the 2<sup>nd</sup> largest area (Fig.  
457 8). In the Willow River Watershed, LSU L1 contributed 16.8% of the total nitrogen  
458 with the 2<sup>nd</sup> largest area, and subbasin S1 contributed 31.7% of total nitrogen which  
459 haswith the 2<sup>nd</sup> largest area of all subbasins (Fig. 9).

460 Although absolute differences exist in the results of the two watersheds due to  
461 different geographic characteristics, the comparison between them is less important for  
462 the scope of this study (which is to evaluate the effectiveness of the PMAs at the LSU  
463 level). Instead, the similar appearance depicted by the relations between the area of  
464 PMAs and their total load contribution at the two levels in different watersheds can also  
465 show the universality and effectiveness of LSUs. In summary, identifying PMAs based  
466 on landscape positions performs better than subbasins from the perspectives of both the  
467 spatial distribution and cumulative load contribution in both test watersheds. Thus,  
468 LSU-based PMAs have the merit of accounting for more pollutant load contributions  
469 with smaller areas, and can effectively be utilized in the spatial configuration of BMPs  
470 for integrated watershed management.

## 471 **5. Conclusions**

472 This study proposes the use of landscape position units (LSUs), derived from a

473 universal type of spatial unit for most geographic environments, as identification units  
474 for priority management areas (PMAs). An ~~improved~~ Markov chain-based surrogate  
475 model of the SWAT<sup>+</sup> model was implemented with the improvement of the transition  
476 matrix in representing both landscape position and channel units to distinguish the  
477 pollutant load contribution of each LSU to the assessment outlet and then identify the  
478 PMAs according to a classification method. ~~Experimental~~ The experimental results  
479 show that landscape position units are more effective than widely used subbasins in  
480 identifying PMAs because of their superior ability to represent hillslope processes and  
481 the spatial heterogeneity of underlying surface environments within subbasins.  
482 Therefore, LSU-based PMAs are much more valuable for providing accurate locations  
483 for implementing suitable BMPs for integrated watershed management.

484 The improved Markov chain-based PMA identification method can be regarded as  
485 a method framework. More types of spatial units with explicit upstream-downstream  
486 relationships may be proposed and validated to identify PMAs with the support of  
487 proper watershed models. In addition, several issues may be worth attention in future  
488 research such as 1) how to consider various climate scenarios to determine the retention  
489 effects of channel routing processes; 2) how to better quantify the hydrological  
490 connectivity among landscape positions and channels and its effects on PMA  
491 identification; 3) how a specific type of identification unit affects the PMA identification  
492 of PMAs under different delineation methods; 4) how the modeling accuracy ~~and~~  
493 precision of the same or different watershed models affects PMA identification; and 5)  
494 how PMAs derived from different identification units impact the effectiveness and

495 efficiency of the spatial optimization of BMPs.

## 496 **Acknowledgements**

497 Supports ~~to~~ for A-Xing Zhu through the Vilas Associate Award, the Hammel Faculty  
498 Fellow Award, and the Manasse Chair Professorship from the University of Wisconsin-  
499 Madison are greatly appreciated.

## 500 **Funding**

501 The work reported here was supported by grants from National Natural Science  
502 Foundation of China (Project No.: 41871362, 42101480, 41871300), [Key Project of](#)  
503 [Innovation LREIS \(Project No.: KPI003\)](#), and the 111 Program of China (Approved  
504 Number: D19002).

## 505 **References**

- 506 Almendinger, J.E., Murphy, M.S., 2007. *Constructing a SWAT model of the Willow River watershed,*  
507 *western Wisconsin. St. Croix Watershed Research Station, Science Museum of Minnesota. 84 pp.*
- 508 Arnold, J., Allen, P., Volk, M., Williams, J.R., Bosch, D., 2010. Assessment of different representations  
509 of spatial variability on SWAT model performance. *Transactions of the ASABE*. 53(5), 1433–1443.  
510 <https://doi.org/10.13031/2013.34913>.
- 511 Bieger, K., Arnold, J.G., Rathjens, H., White, M.J., Bosch, D.D., Allen, P.M., 2019. Representing the  
512 connectivity of upland areas to floodplains and streams in SWAT+. *J. Am. Water Resour. Assoc.*  
513 55(3), 578–590. <https://doi.org/10.1111/1752-1688.12728>.
- 514 Bieger, K., Arnold, J.G., Rathjens, H., White, M.J., Bosch, D.D., Allen, P.M., Volk, M., Srinivasan, R.,  
515 2017. Introduction to SWAT+, a completely restructured version of the Soil and Water Assessment

516 Tool. *J. Am. Water Resour. Assoc.* 53(1), 115–130. <https://doi.org/10.1111/1752-1688.12482>.

517 Chen, L., Li, J., Xu, J., Liu, G., Wang, W., Jiang, J., Shen, Z., 2022. New framework for nonpoint source  
518 pollution management based on downscaling priority management areas. *J. Hydrol.* 606, 127433.  
519 <https://doi.org/10.1016/j.jhydrol.2022.127433>.

520 Chen, L., Zhong, Y., Wei, G., Cai, Y., Shen, Z., 2014. Development of an integrated modeling approach  
521 for identifying multilevel non-point-source priority management areas at the watershed scale. *Water  
522 Resour. Res.* 50(5), 4095–4109. <https://doi.org/10.1002/2013WR015041>.

523 Chiang, L.C., Chaubey, I., Maringanti, C., Huang, T., 2014. Comparing the selection and placement of  
524 best management practices in improving water quality using a multiobjective optimization and  
525 targeting method. *Int. J. Environ. Res. Public Health* 11(3), 2992–3014.  
526 <https://doi.org/10.3390/ijerph110302992>.

527 [De Smith, M. J., Goodchild, M. F., Longley, P., 2018. \*Geospatial analysis: A comprehensive guide to\*  
528 \*principles, techniques and software tools\*. 6th edition, England: The Winchelsea Press.](#)

529 Dong, F., Liu, Y., Wu, Z., Chen, Y., Guo, H., 2018. Identification of watershed priority management areas  
530 under water quality constraints: A simulation-optimization approach with ideal load reduction. *J.  
531 Hydrol.* 562, 577–588. <https://doi.org/10.1016/j.jhydrol.2018.05.033>.

532 Engel, B., Storm, D., White, M., Arnold, J., Arabi, M., 2007. A hydrologic/water quality model  
533 application protocol. *J. Am. Water Resour. Assoc.* 43(5), 1223–1236. [https://doi.org/10.1111/j.1752-  
534 1688.2007.00105.x](https://doi.org/10.1111/j.1752-1688.2007.00105.x).

535 ~~[U.S. Environmental Protection Agency. EPA, 2022. U.S. Environmental Protection Agency. Level III](#)  
536 [and IV ecoregions of the continental environmental probability. Available online at](#)  
537 <https://www.epa.gov/eco-research/level-iii-and-iv-ecoregions-state>, last updated on May 2, 2022.~~

538 Ghebremichael, L.T., Veith, T.L., Hamlett, J.M., 2013. Integrated watershed- and farm-scale modeling  
539 framework for targeting critical source areas while maintaining farm economic viability. *J. Environ.*  
540 *Manage.* 114, 381–394. <https://doi.org/10.1016/j.jenvman.2012.10.034>.

541 Giri, S., Qiu, Z., Prato, T., Luo, B., 2016. An integrated approach for targeting critical source areas to  
542 control nonpoint source pollution in watersheds. *Water Resour. Manage.* 30, 5087–5100.  
543 <https://doi.org/10.1007/s11269-016-1470-z>.

544 Grimvall, A., Stålnacke, P., 1996. Statistical methods for source apportionment of riverine loads of  
545 pollutants. *Environmetrics* 7(2), 201–213. [https://doi.org/10.1002/\(SICI\)1099-095X\(199603\)7:2<201::AID-ENV205>3.0.CO;2-R](https://doi.org/10.1002/(SICI)1099-095X(199603)7:2<201::AID-ENV205>3.0.CO;2-R).

547 Guo, Y., Wang, X., Melching, C., Nan, Z., 2022. Identification method and application of critical load  
548 contribution areas based on river retention effect. *J. Environ. Manage.* 305, 114314.  
549 <https://doi.org/10.1016/j.jenvman.2021.114314>.

550 Hejzlar, J., Anthony, S., Arheimer, B., Behrendt, H., Bouraoui, F., Grizzetti, B., Groenendijk, P., Jeuken,  
551 M.H.J.L., Johnsson, H., Lo Porto, A., Kronvang, B., Panagopoulos, Y., Siderius, C., Silgram, M.,  
552 Venohr, M., Žaloudík, J., 2009. Nitrogen and phosphorus retention in surface waters: ~~an~~ [An](#) inter-  
553 comparison of predictions by catchment models of different complexity. *J. Environ. Monit.* 11(3),  
554 584. <https://doi.org/10.1039/b901207a>.

555 Kovacs, A., Honti, M., Zessner, M., Eder, A., Clement, A., Blöschl, G., 2012. Identification of  
556 phosphorus emission hotspots in agricultural catchments. *Sci. Total Environ.* 433, 74–88.  
557 <https://doi.org/10.1016/j.scitotenv.2012.06.024>.

558 Liu, G., Chen, L., Wei, G., Shen, Z., 2019. New framework for optimizing best management practices at  
559 multiple scales. *J. Hydrol.* 578, 124133. <https://doi.org/10.1016/j.jhydrol.2019.124133>.

560 Miller, B.A., Schaetzl, R.J., 2015. Digital classification of hillslope position. *Soil Sci. Soc. Am. J.* 79(1),  
561 132–145. <https://doi.org/10.2136/sssaj2014.07.0287>.

562 Moriasi, D. N., Arnold, J. G., Van Liew, M. W., Bingner, R. L., Harmel, R. D., Veith, T. L., 2007. Model  
563 evaluation guidelines for systematic quantification of accuracy in watershed simulations.  
564 *Transactions of the ASABE*. 50(3), 885–900. <https://doi.org/10.13031/2013.23153>.

565 Nash, J.E., Sutcliffe, J.V., 1970. River flow forecasting through conceptual models part I — A discussion  
566 of principles. *J. Hydrol.* 10(3), 282–290. [https://doi.org/10.1016/0022-1694\(70\)90255-6](https://doi.org/10.1016/0022-1694(70)90255-6).

567 [Neitsch, S. L., Arnold, J. G., Kiniry, J. R., & Williams, J. R., \(2011\). Soil and water assessment tool](#)  
568 [theoretical documentation version 2009. Texas Water Resources Institute.](#)

569 Pionke, H.B., Gburek, W.J., Sharpley, A.N., 2000. Critical source area controls on water quality in an  
570 agricultural watershed located in the Chesapeake Basin. *Ecol. Eng.* 14(4), 325–335.  
571 [https://doi.org/10.1016/S0925-8574\(99\)00059-2](https://doi.org/10.1016/S0925-8574(99)00059-2).

572 Qin, C.-Z., Gao, H.-R., Zhu, L.-J., Zhu, A.-X., Liu, J.-Z., Wu, H., 2018. Spatial optimization of watershed  
573 best management practices based on slope position units. *J. Soil Water Conserv.* 73(5), 504–517.  
574 <https://doi.org/10.2489/jswc.73.5.504>.

575 [Qin, C.-Z., Zhu, A.-X., Shi, X., Li, B.-L., Pei, T., Zhou, C.-H., 2009. Quantification of spatial gradation](#)  
576 [of slope positions. \*Geomorphology\* 110, 152–161. <https://doi.org/10.1016/j.geomorph.2009.04.003>](#)

577 Rankinen, K., Keinänen, H., Cano Bernal, J.E., 2016. Influence of climate and land use changes on  
578 nutrient fluxes from Finnish rivers to the Baltic Sea. *Agr. Ecosyst. Environ.* 216, 100–115.  
579 <https://doi.org/10.1016/j.agee.2015.09.010>.

580 Rathjens, H., Bieger, K., Chaubey, I., Arnold, J.G., Allen, P.M., Srinivasan, R., Bosch, D.D., Volk, M.,  
581 2016. Delineating floodplain and upland areas for hydrologic models: a comparison of methods.

582 Hydrol. Process. 30(23), 4367–4383. <https://doi.org/10.1002/hyp.10918>.

583 Rathjens, H., Oppelt, N., Bosch, D.D., Arnold, J.G., Volk, M., 2015. Development of a grid-based version  
584 of the SWAT landscape model. Hydrol. Process. 29(6), 900–914. <https://doi.org/10.1002/hyp.10197>.

585 Shang, X., Wang, X., Zhang, D., Chen, W., Chen, X., Kong, H., 2012. An improved SWAT-based  
586 computational framework for identifying critical source areas for agricultural pollution at the lake  
587 basin scale. Ecol. Model. 226, 1–10. <https://doi.org/10.1016/j.ecolmodel.2011.11.030>.

588 Shen, Z., Zhong, Y., Huang, Q., Chen, L., 2015. Identifying non-point source priority management areas  
589 in watersheds with multiple functional zones. Water Res. 68, 563–571.  
590 <https://doi.org/10.1016/j.watres.2014.10.034>.

591 Shi, Y.-X., Zhu, L.-J., Qin, C.-Z., Zhu, A.-X., 2021. Spatial optimization of watershed best management  
592 practices based on slope position-field units. Journal of Geo-Information Science 23(4), 564–575.  
593 (in Chinese with English abstract). <https://doi.org/10.12082/dqxxkx.2021.200335>.

594 Tian, F., Huang, J., Cui, Z., Gao, J., Wang, X., Wang, X., 2020. Integrating multi indices for identifying  
595 priority management areas in lowland to control lake eutrophication: A case study in lake Gehu,  
596 China. Ecol. Indic. 112, 106103. <https://doi.org/10.1016/j.ecolind.2020.106103>.

597 Volk, M., Arnold, J.G., Bosch, D.D., Allen, P.M., Green, C.H., 2007. Watershed configuration and  
598 simulation of landscape processes with the SWAT model, in: MODSIM 2007 International Congress  
599 on Modelling and Simulation. Modelling and Simulation Society of Australia and New Zealand,  
600 Christchurch, New Zealand, pp. 2383–2389.

601 Wang, G., Chen, L., Huang, Q., Xiao, Y., Shen, Z., 2016. The influence of watershed subdivision level  
602 on model assessment and identification of non-point source priority management areas. Ecol. Eng.  
603 87, 110–119. <https://doi.org/10.1016/j.ecoleng.2015.11.041>.

604 White, M.J., Storm, D.E., Busteed, P.R., Stoodley, S.H., Phillips, S.J., 2009. Evaluating nonpoint source  
605 critical source area contributions at the watershed scale. *J. Environ. Qual.* 38(4), 1654–1663.  
606 <https://doi.org/10.2134/jeq2008.0375>.

607 Wolock, D.M., Winter, T.C., McMahon, G., 2004. Delineation and evaluation of hydrologic-landscape  
608 regions in the United States using geographic information system tools and multivariate statistical  
609 analyses. *Environ. Manage.* 34, S71–S88. <https://doi.org/10.1007/s00267-003-5077-9>.

610 [U.S. Environmental Protection Agency. \(EPA\). 2022. Level III and IV ecoregions of the continental](https://www.epa.gov/eco-research/level-iii-and-iv-ecoregions-state)  
611 [environmental probability. Available online at https://www.epa.gov/eco-research/level-iii-and-iv-](https://www.epa.gov/eco-research/level-iii-and-iv-ecoregions-state)  
612 [ecoregions-state. last updated on May 2, 2022.](https://www.epa.gov/eco-research/level-iii-and-iv-ecoregions-state)

613 Yang, D., Herath, S., Musiake, K., 2002. A hillslope-based hydrological model using catchment area and  
614 width functions. *Hydrolog. Sci. J.* 47(1), 49–65. <https://doi.org/10.1080/02626660209492907>.

615 Zhu, L.-J., Qin, C.-Z., Zhu, A.-X., 2021. Spatial optimization of watershed best management practice  
616 scenarios based on boundary-adaptive configuration units. *Progress in Physical Geography: Earth*  
617 *and Environment* 45(2), 207–227. <https://doi.org/10.1177/0309133320939002>.

618 Zhu, L.-J., Qin, C.-Z., Zhu, A.-X., Liu, J., Wu, H., 2019. Effects of different spatial configuration units  
619 for the spatial optimization of watershed best management practice scenarios. *Water* 11(2), 262.  
620 <https://doi.org/10.3390/w11020262>.



## Table

**Table 1. Data description of the study areas for building a SWAT+ [model](#).**

	Zhongtianshe Watershed	Willow River Watershed
DEM	DEM with a resolution of 25 m from Provincial Geomatics Centre of Jiangsu	DEM with a resolution of 30 m from National Elevation Data, USGS
Land use	Manually interpreted from <a href="#">a Google Earth</a> image derived in 2015	Land use map from National Land Cover Data (NLCD, 2011 Edition), USGS
Soil	Soil type map obtained from Soil Science Database of China and soil properties from field sampling	Soil dataset from the Soil Survey Geographic database (SSURGO), U.S. Department of Agriculture-Natural Resource Conservation Service
Meteorological data	Daily meteorological data (such as precipitation, temperature, humidity, wind speed, and solar radiation) from 2011 to 2015 provided by China Meteorological Data Service Centre and Liyang <a href="#">meteorological Meteorological station</a>	Daily meteorological data from 2008 to 2014 provided by Climate Forecast System Reanalysis <a href="#">datasetDataset</a> , U.S. National Centers for Environmental Prediction
Agricultural management practices	Cropping and irrigation schedule including crop types and fertilizer usage from field survey	Crop rotations, tillage practices, and fertilizer usage collated from Almendinger and Murphy (2007)
Observed data at the outlet	Daily measured flow (2011–2015) and 5-day <a href="#">or 3-day*</a> measured total nitrogen data (2014–2015) from the site-monitoring station at the watershed outlet	Daily flow and ammonia plus organic nitrogen data (from 1 October 2010 to 31 July 2014) measured at the monitoring station <a href="#">by of the</a> USGS (no. 05341687)

[\\* A total of 181 values were monitored in the Zhongtianshe watershed. During the rainy season \(i.e., June to August\), the sampling interval is about three days.](#)

**Table 2. The SWAT<sup>+</sup> model performance ~~of~~for the two study watersheds.**

			NSE	PBIAS	RSR	R <sup>2</sup>
Zhongtianshe Watershed	Calibration	Flow	0.48	13.36%	0.72	0.52
		Nitrogen	0.27	-16.57%	0.86	0.40
	Validation	Flow	0.52	12.55%	0.69	0.59
		Nitrogen	–	–	–	–
Willow River Watershed	Calibration	Flow	0.48	-28.82%	0.72	0.51
		Nitrogen	0.37	3.97%	0.79	0.39
	Validation	Flow	0.34	-58.16%	0.81	0.47
		Nitrogen	0.25	-128.73%	0.87	0.54

**Figure**

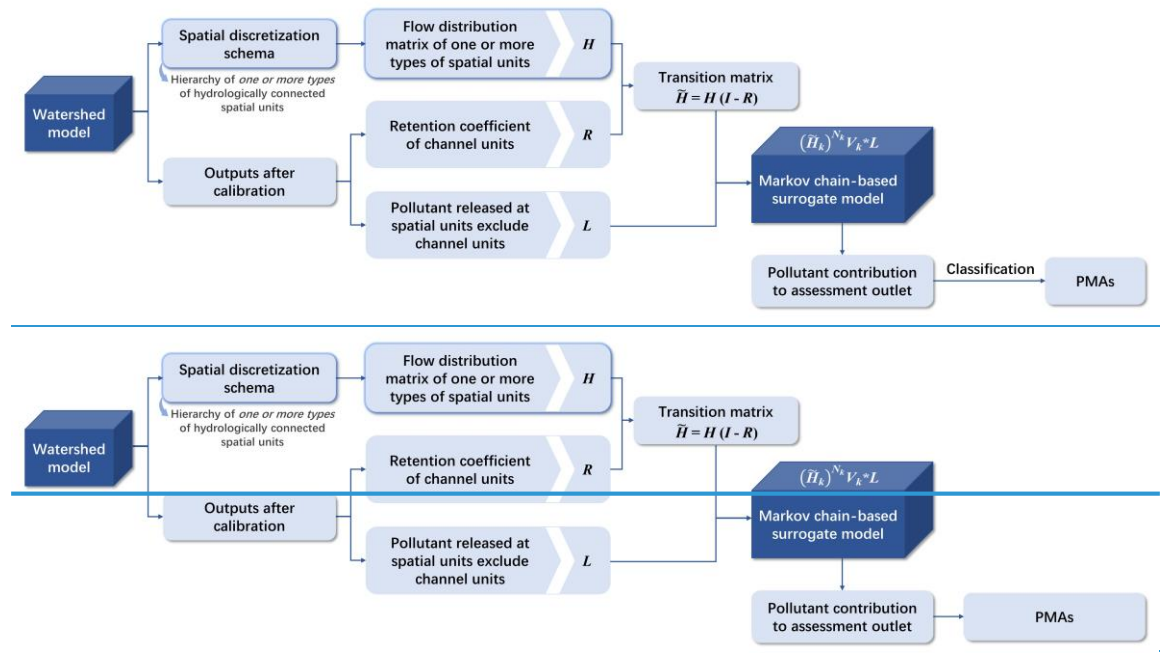


**Fig. 1. Generalized framework of the Markov chain-based PMA identification method using a hierarchy of one or more types of hydrologically connected spatial units.**

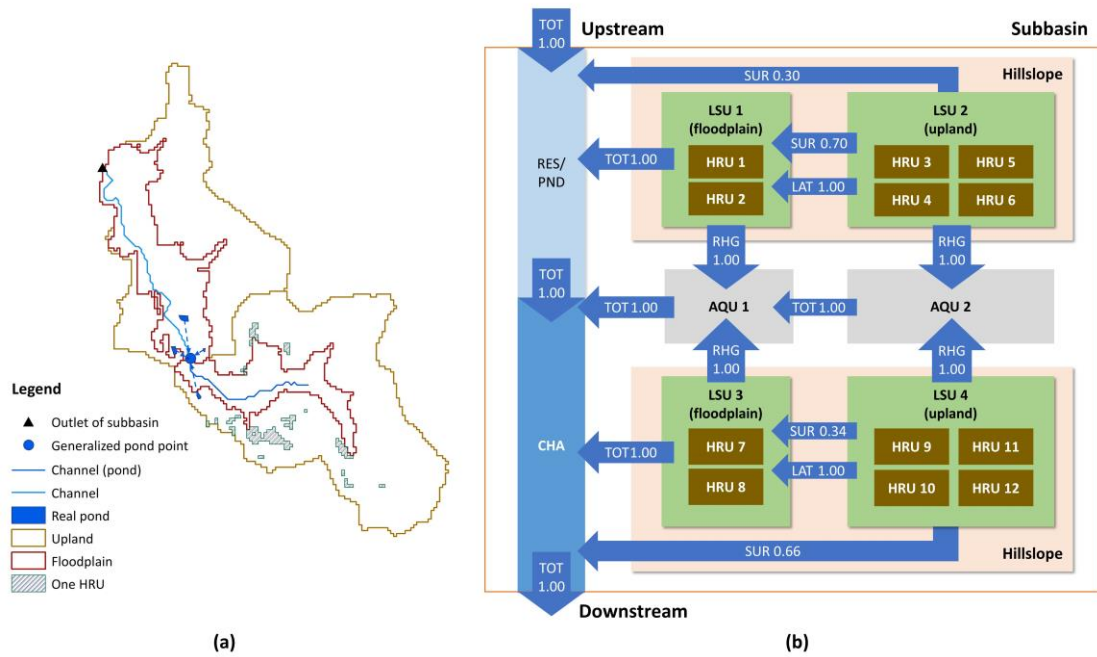


**Fig. 2.** Schematic of the spatial discretization scheme (a) and hydrologic connections between spatial units (b) implemented in SWAT+. AQU, aquifer; CHA, channel; HRU, hydrologic response unit; LSU, landscape position unit; LAT, lateral flow; PND, pond; RES, reservoir; RHG, groundwater recharge; SUR, surface runoff; TOT, total outflow (specifically, for LSU, it equals to surface runoff plus lateral flow); and numbers represent flow distribution ratio (values less than 1.0 are presented for example) from source unit to receiving unit (adapted from Bieger et al., 2017, 2019, and the source code of SWAT+ version 59.3).

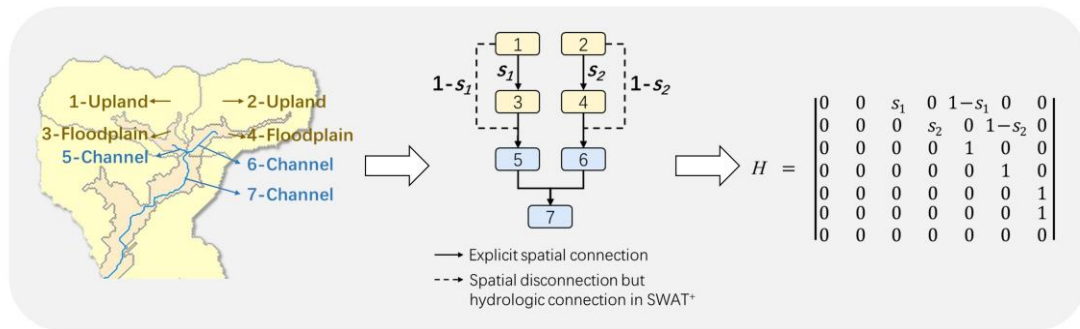


**Fig. 3. Example of constructing construction of the flow distribution matrix,  $H_2$ , based on upstream-downstream relationships among landscape position units (LSUs) and channels and flow distribution ratios from upland to floodplain (e.g.,  $s_1$  and  $s_2$  in different subbasins).**

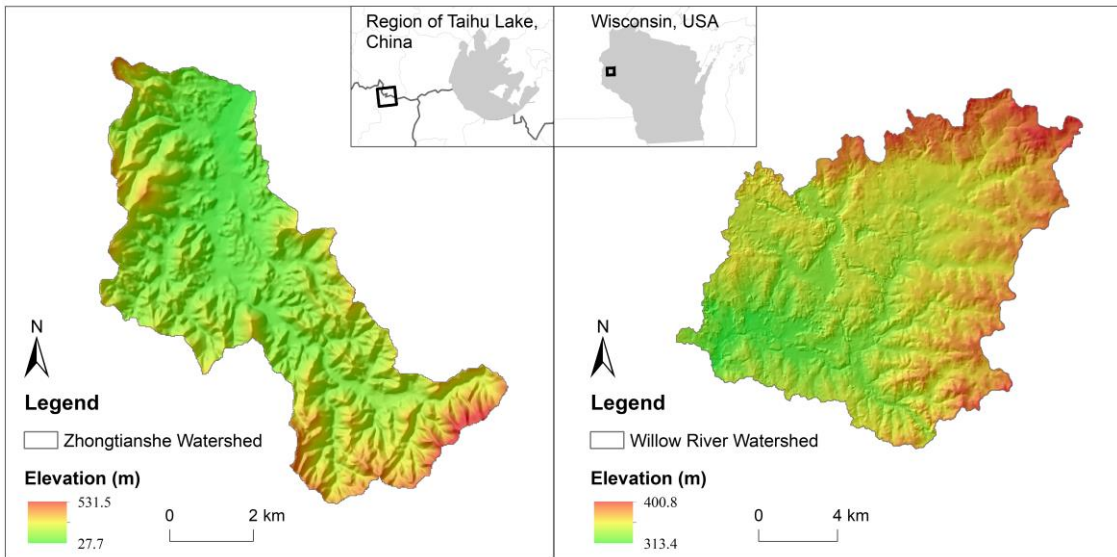
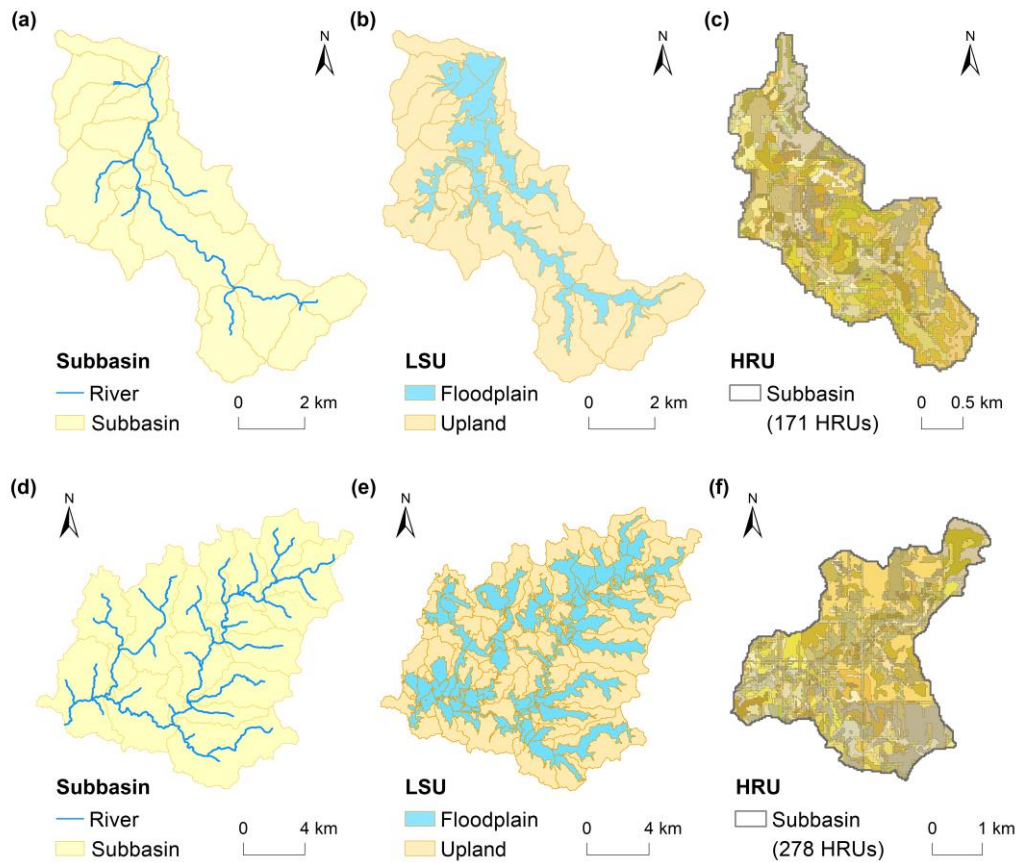
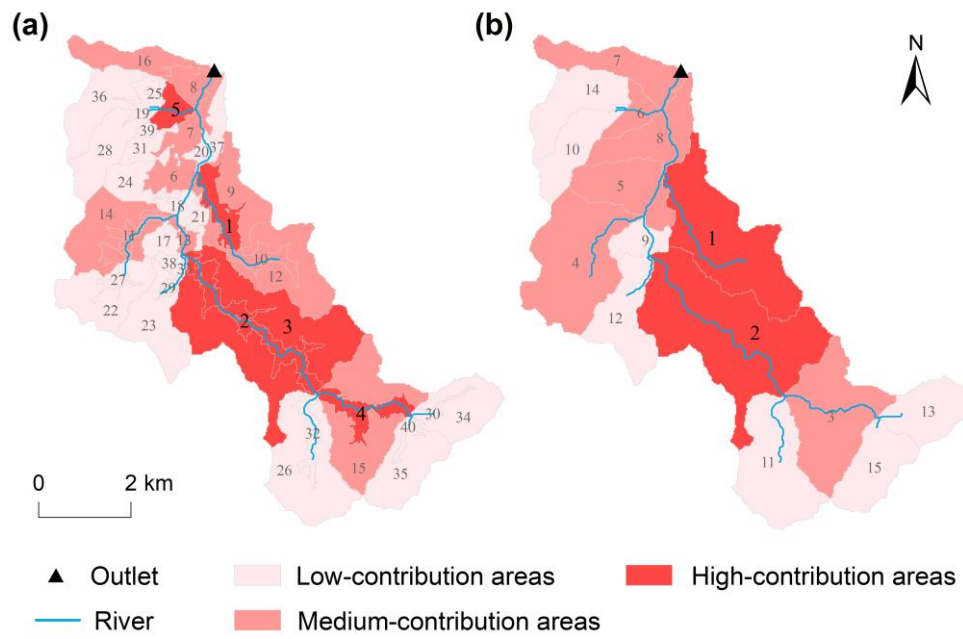


Fig. 4. Overview of the Zhongtianshe and Willow River [Watersheds](#).



**Fig. 5. Delineation of three types of spatial units in the SWAT<sup>+</sup> model of the Zhongtianshe Watershed: (a) subbasin, (b) LSU, and (c) HRU (~~take-taking~~ one subbasin as an example); and the Willow River Watershed: (d) subbasin, (e) LSU, and (f) HRU (~~take-taking~~ one subbasin as an example). Each color within the same subbasin in the HRU map represents one unit, i.e., a particular combination of land use, soil type, and slope classification.**



**Fig. 6. Ranking and classification of nitrogen load contribution at the (a) LSU (landscape position unit) and (b) subbasin levels in the Zhongtianshe Watershed. The labelled number is the ranked sequence of load contribution in descending order. High-contribution areas are identified as PMAs.**



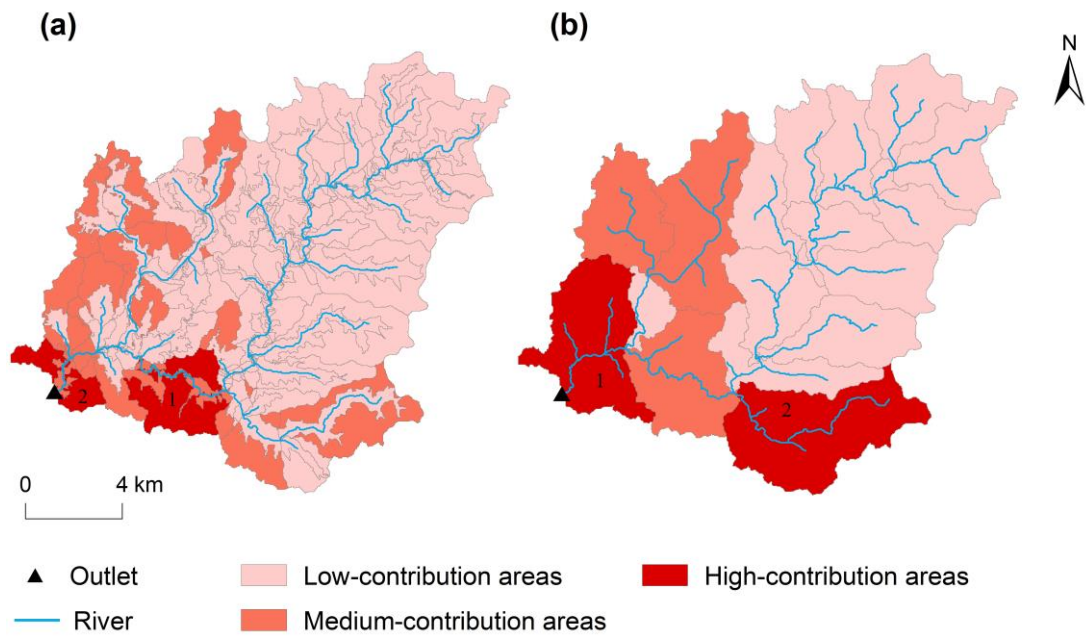


**Fig. 7. Ranking and classification of total nitrogen load contribution at the (a) LSU (landscape position unit) and (b) subbasin levels in the Willow River Watershed. High-contribution areas are identified as PMAs, which are ranked and labelled by load contribution.**

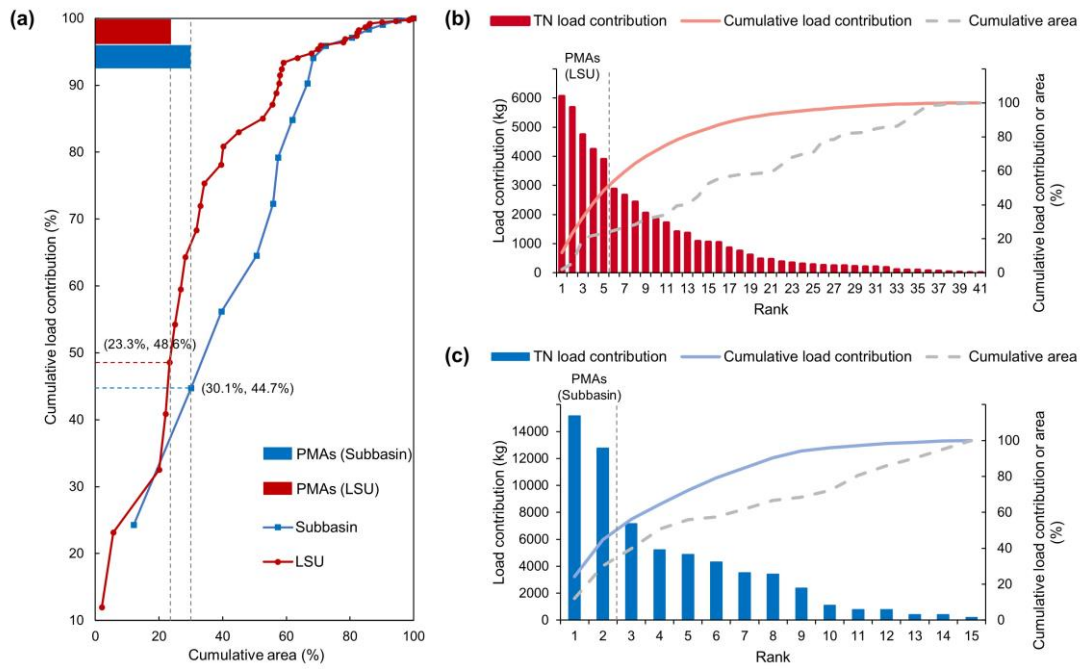


**Fig. 8. Relationships** between cumulative areas of spatial units and corresponding load contributions in the Zhongtianshe Watershed. (a) each point represents a spatial unit arranged in the descending order of load contribution. Detailed load contribution of landscape position units (LSUs) and subbasins are presented in (b) and (c), respectively.

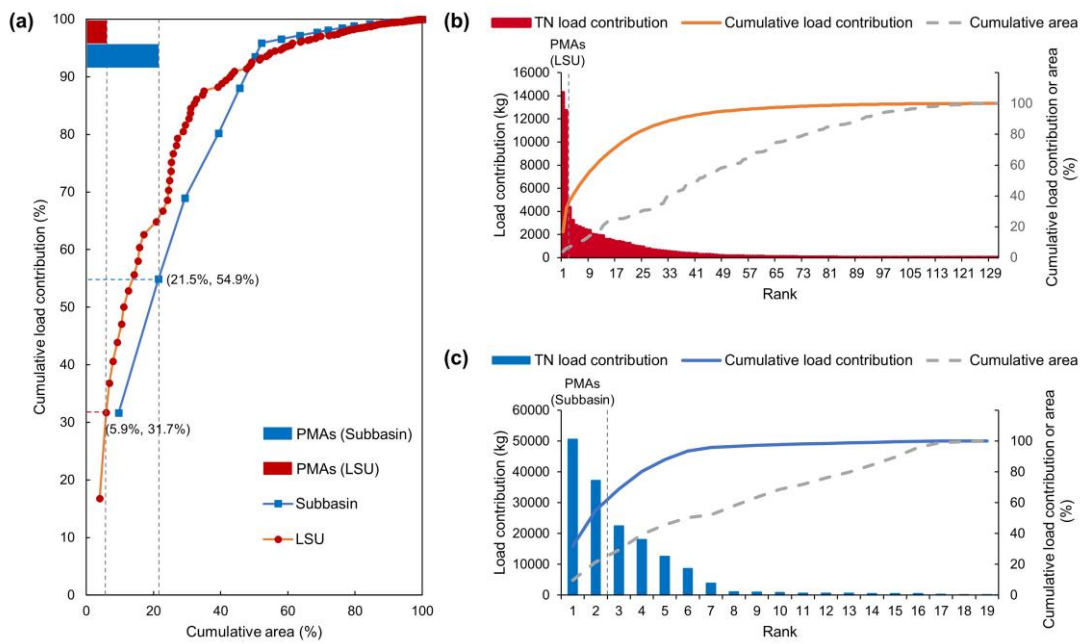


**Fig. 9. Relationships** between cumulative areas of spatial units and corresponding load contributions in the Willow River Watershed. (a) each point represents a spatial unit arranged in the descending order of load contribution. Detailed load contribution of landscape position units (LSUs) and subbasins are presented in (b) and (c), respectively.